Illuminating Basement Structure Using 3D Seismic and Potential Field Data, Arkoma Basin, Oklahoma and Arkansas

ConocoPhillips School of Geology & Geophysics, The University of Oklahoma

Hamed Alrefaee, Kurt J. Marfurt and Randy G. Keller, University of Oklahoma

Abstract

We have used three dimensional (3D) seismic, magnetic, and gravity data in an integrated approach to map the basement surface and the associated structural features in the Arkoma basin, Oklahoma and Arkansas. The structural interpretation and seismic attributes have revealed an EW striking zone of intensive deformation or crustal weakness at the northern part of the study area. The weakness zone may represent a Late Paleozoic tectonic (structural) inversion of the normal faulting (block faulting) which developed during the Cambrian rifting. The structural interpretation reveals also a compressive structural style of deformation related to Ouachita orogeny dominating the Late Paleozoic time. We have recognized a clear relationship between the Precambrian basement structures and the Paleozoic structural deformation and depositional history. Edge detector techniques of the magnetic data have delineated clear magnetic boundaries (faults or body edges) that extend in EW, NE-SW and NW-SE in the northern, southeastern, and western parts of the study area, respectively. Euler magnetic depth estimation method has also delineated the previously mentioned faults by showing clustering of the solutions along these fault trends. Euler's method shows a maximum depth value of about 3850 m to the faults that affect the basement and/or the intrabasement features. The trends of the faults obtained from seismic data interpretation show a remarkably clear correlation with those determined by the Euler's method and the edge detector techniques.

Regional Geology and Tectonic Setting

Arkoma basin is an arcuate structural feature that extends from the Gulf coastal plain in central Arkansas westward to the Arbuckle Mountains in south-central Oklahoma. The basin was once a part of the large Ouachita geosyncline and it has been developed as a foreland basin related to Ouachita Orogeny Fig. (1). Rocks in the basin have been highly deformed by a combination of forces. Tensional forces during the basin subsidence developed normal faults and major block faulting at deeper levels Figs. (2&3). Compressive horizontal forces related to the Ouachita orogeny has developed folds and thrust faults at shallower levels. Sedimentary rocks in Arkoma basin range in thickness from 3,000 to 20,000 ft. and consist primarily of pre Mississippian carbonate shelf deposits, organic-rich Mississippian marine shale and Pennsylvanian fluvial deposits Fig. (4).

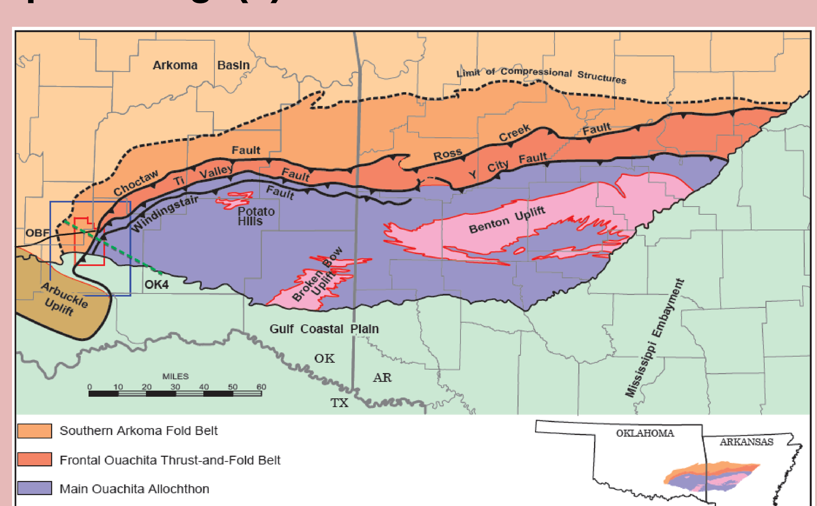

Fig. (1). Index map of the study area showing the main structural provinces of the Arkoma basin-Ouachita orogenic belt province. The blue rectangle shows the boundary of the total magnetic intensity map, and the red polygon shows the boundary of the 3D seismic survey. OBF refers to the Olney-Bromide fault, and OK4 refers to structural cross section shown in dashed green color across the study area, (Modified from Arbenz, 2008).

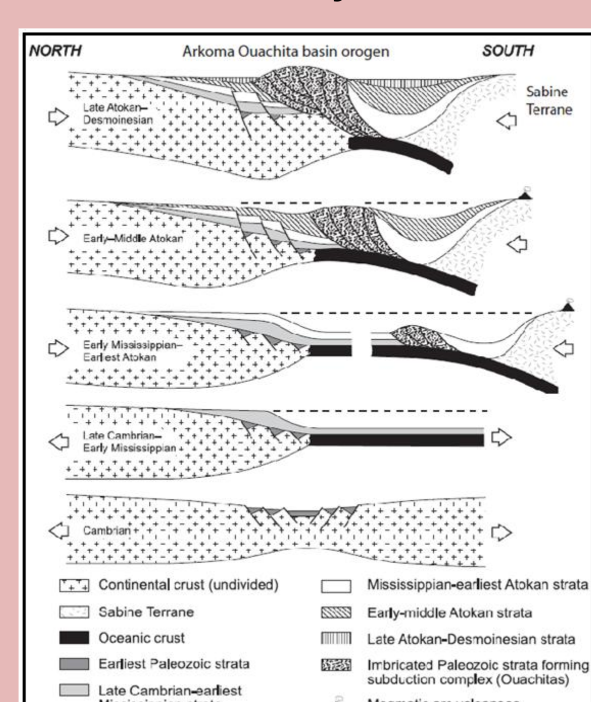

Fig. (2). Tectonic evolution of Arkoma basin and Ouachita orogenic belt from Keller (2009) after Houseknect and Mathews (1985).

Study Area

The study area is located at the most western part of the Arkoma basin in south eastern Oklahoma where it is bounded by Arbuckle uplift to the west. The area occupied part of the transition zone between the Ouachita frontal zone and Arkoma basin.

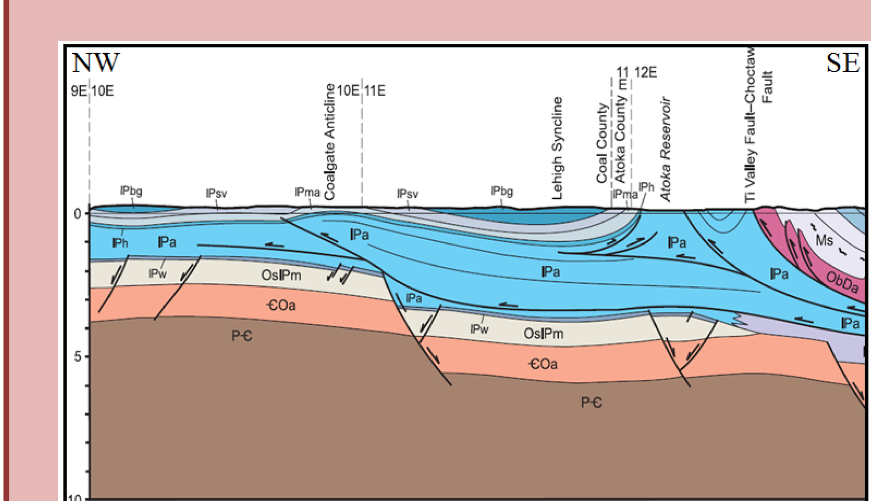

Fig. (3). Structural cross section OK4 across Ouachita Orogenic belt. The cross section shows the tectonic evolution of the Arkoma basin and Ouachita orogenic belt, modified after Arbenz, 2008.

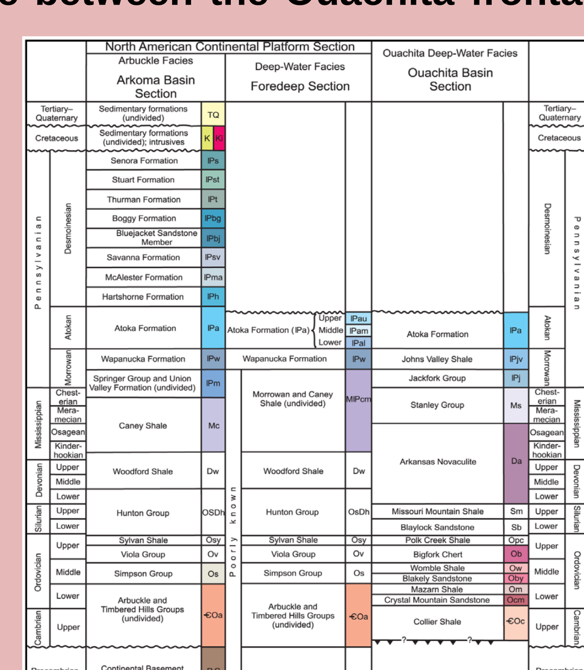

Fig. (4). Stratigraphic section of Arkoma basin-Ouachita orogenic belt province from Arbenz (2008).

3D Seismic Data

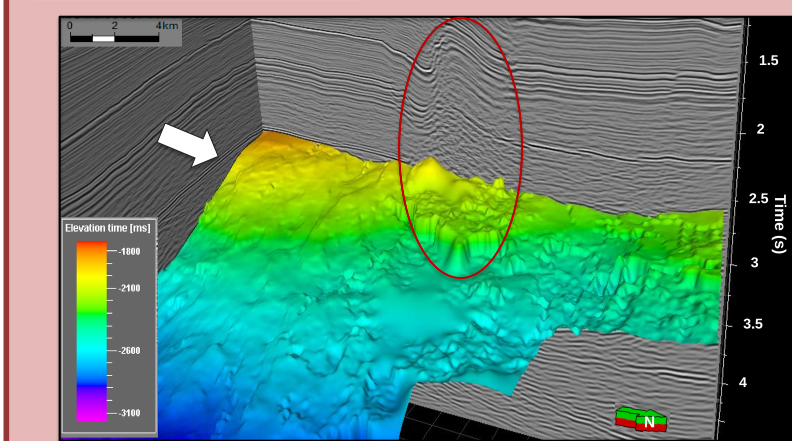

Fig. (5). 3D view showing the basement surface with intensive deformation due to tectonic inversion. The white arrow shows an unconformity surface between the basement and the Lower Paleozoic strata. The red ellipse shows an area of severe deformation.

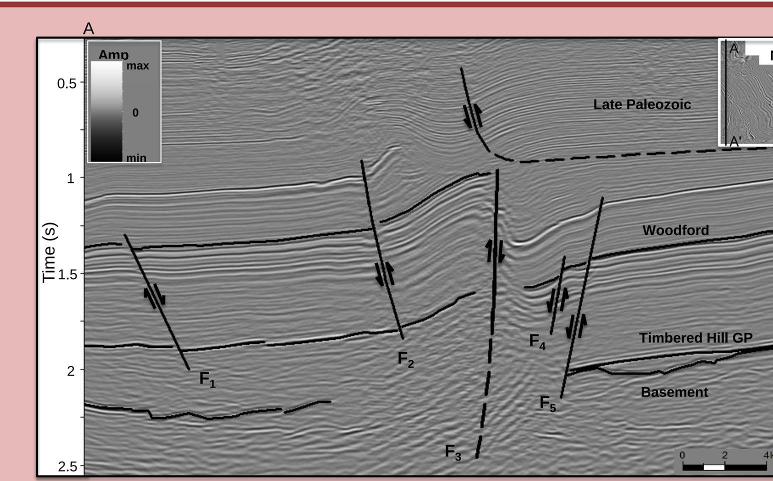

Fig. (6). Seismic section AA' showing an area of intensive deformation where some basement normal faults were reactivated as reverse faults (F2 and F3). The shallower Late Paleozoic thrust fault align vertically above the deeper basement fault. A distinct thickening of the Late Paleozoic strata is noticed above the downthrown blocks.

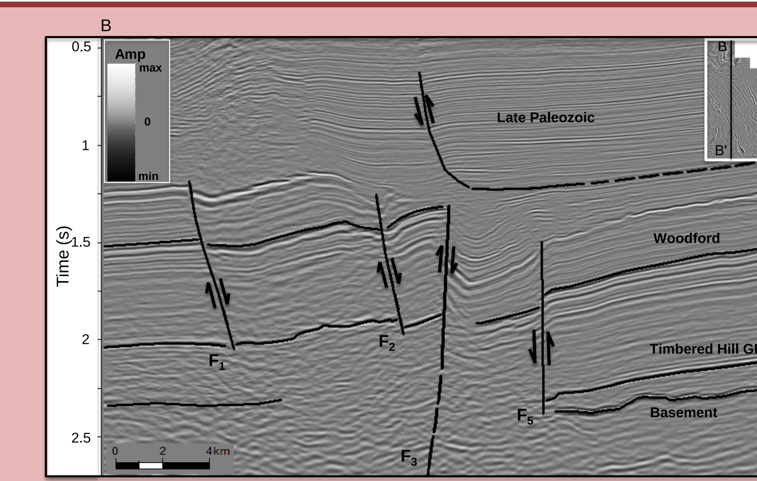

Fig. (7). Seismic section BB' showing the same area of intensive deformation where the master rift fault F3 was reactivated as a reverse fault. The fault F2 is normal in this seismic section. The seismic section BB' shows thicker Late Paleozoic strata above the downthrown blocks than those in the section AA'.

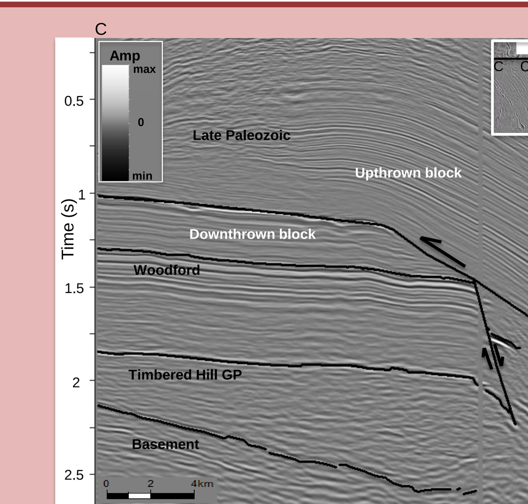

Fig. (8). The seismic section CC' showing the alignment of a thrust fault above the deeper normal fault as well as thickening of the Late Paleozoic strata above the downthrown blocks.

Seismic Attributes Analysis

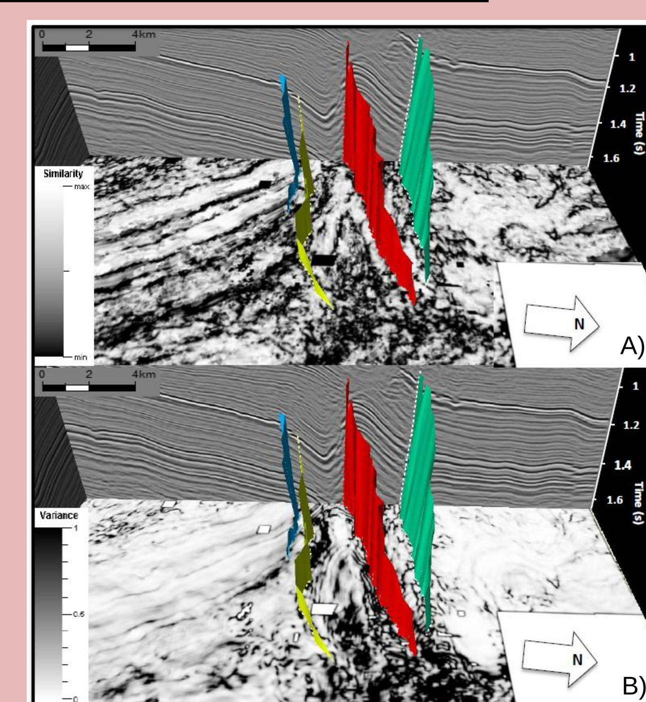

Fig. (9). (A) Time slice (1650 ms) through the coherence volume and (B) time slice at the same level through the variance volume showing the discontinuities (faults and deformed zones) as incoherent black lineaments.

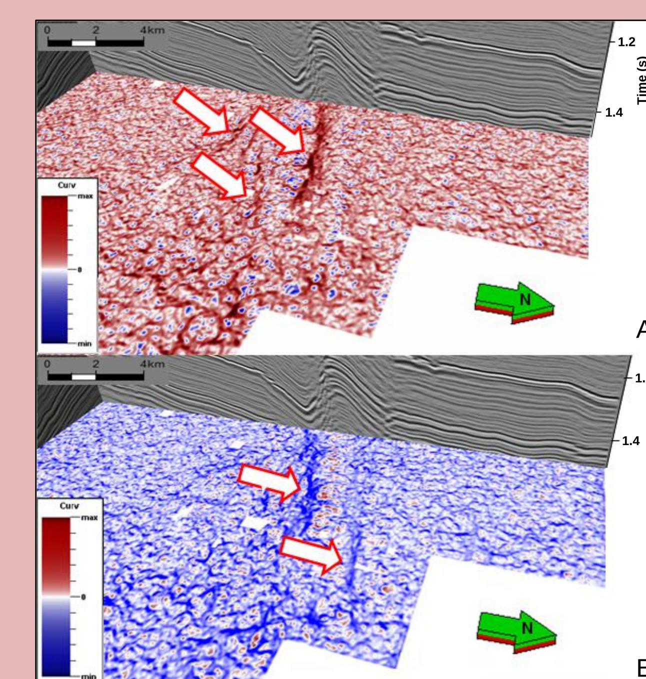

Fig. (10). (A) Time slice (1500 ms) through the most positive curvature volume showing maximum values over the upthrown blocks and the anticlinal features, see the arrows. (B) Time slice (1500 ms) through the most negative curvatures volumes shows maximum values over the downthrown blocks and the synclinal features see the arrows.

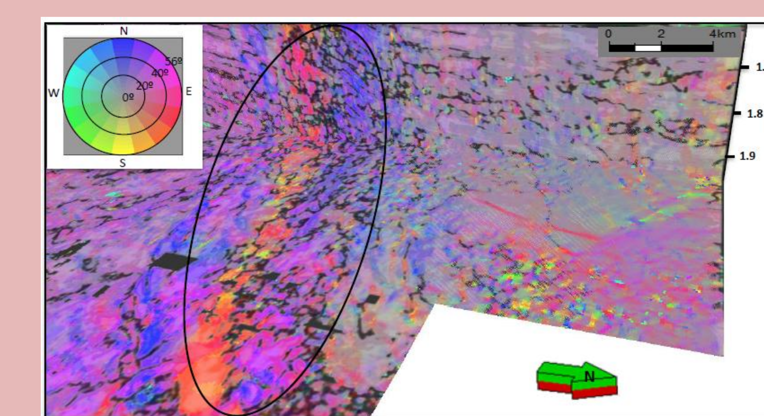

Fig. (11). A three dimensional view through the combined dip magnitude-dip azimuth volume co-rendered with the coherence volume showing an EW trend of high dip angles shown in bright colors corresponding to the area of high dip magnitude (see the ellipse) while the flatter areas are shown in pastel colors.

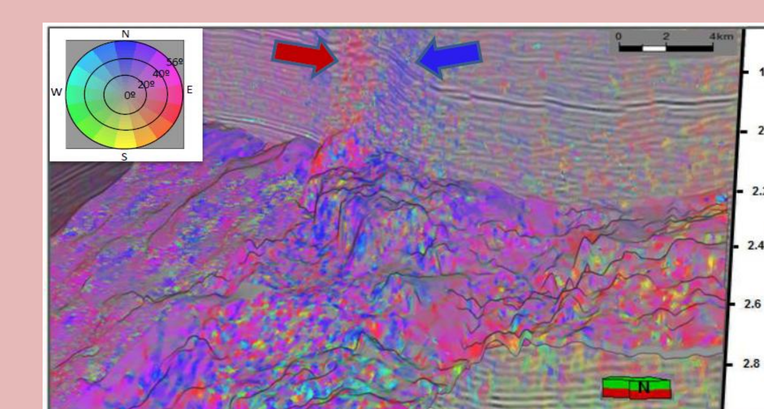

Fig. (12). A combined dip magnitude-dip azimuth volume co-rendered with the seismic volume as well as horizon probe through the basement surface showing an EW trend of high dip angles shown in bright colors corresponding to the area of high deformation while the flatter areas are shown in pastel colors. The downthrown blocks of the basement shows a belt of bright orange to red which indicate dipping to the southeast (red arrow), while the upthrown blocks are shown in blue indicating dip to the north (blue arrow).

Gravity and Magnetic Data Analysis

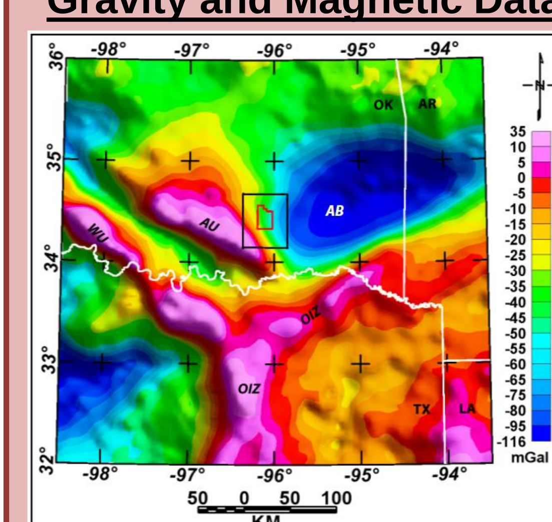

Fig. (13). Bouguer gravity map of Arkoma basin and its surrounding showing very low gravity anomaly related to Arkoma basin (AB) and very high anomalies coinciding with Wichita Uplifts (WU), Arbuckle Uplifts (AU) and Ouachita interior zone (OIZ). The black rectangle shows the boundaries of the total magnetic intensity map and the red polygon shows the boundaries of the seismic survey.

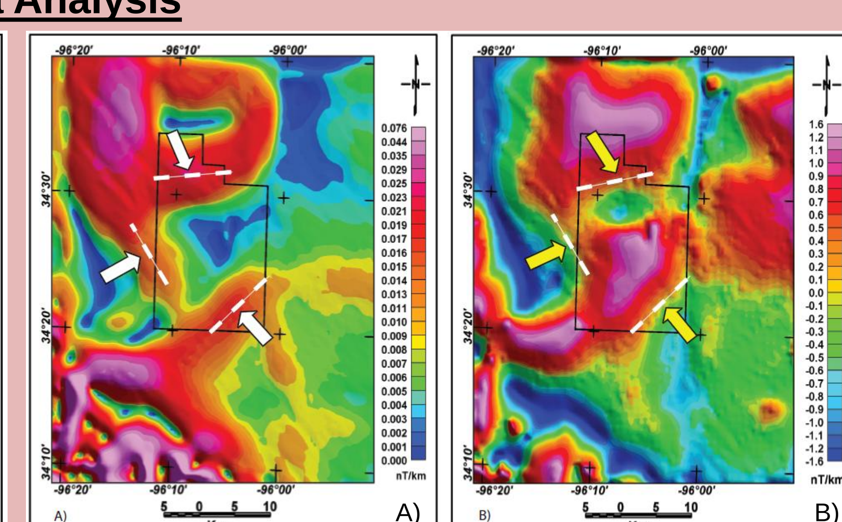

Fig. (14). (A) The total horizontal derivative of the magnetic data showing magnetic maxima above the magnetic edges or the faults, see the white arrows. (B) The tilt derivative showing low or close to zero magnetic values above the edges or the faults and it shows maxima above the body center, see the yellow arrows.

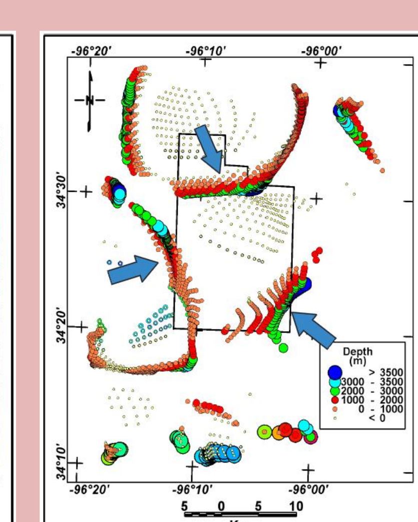

Fig. (15). Euler solution plot using structural index (SI=0.0 faults). The plot shows three clusters along EW trend at the north, NE-SW trend at the southeast, and NW-SE at the west. These clusters coincide with the Olney-Bromide fault, Choctaw fault and unknown fault, respectively, see the blue arrows.

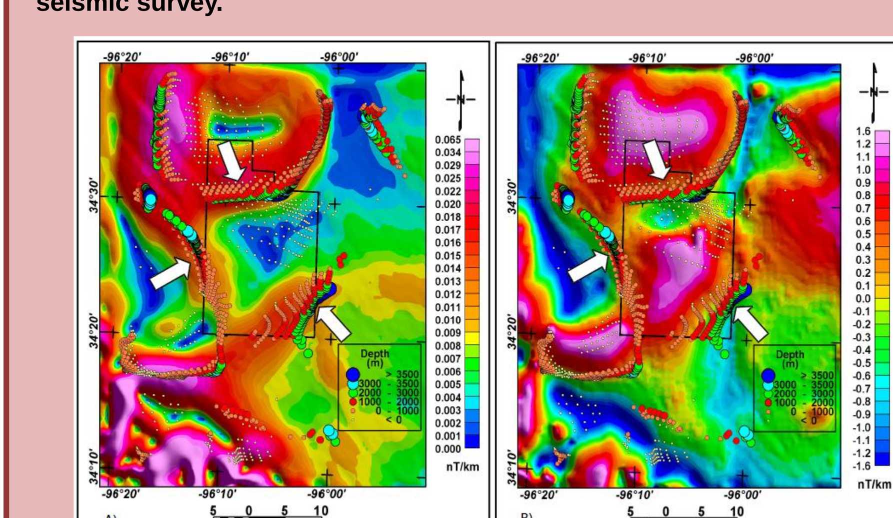

Fig. (16). (A) The Euler solution cluster superimposed on the total horizontal derivative of the magnetic data. (B) The Euler solution cluster superimposed on the tilt derivative. The cluster plots coincide with the fault trends or the edges of the magnetic source bodies, see the white arrows.

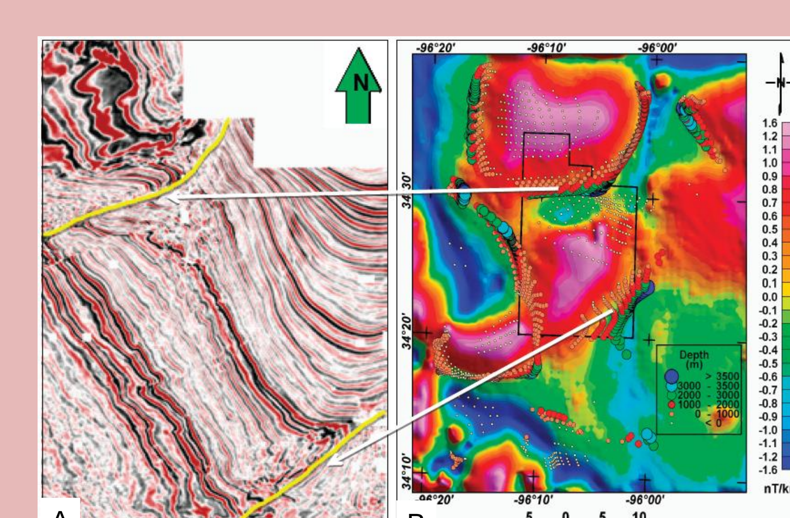

Fig. (17). (A) Time slice (1500) through the seismic volume and (B) the Euler solution cluster plot superimposed on the tilt derivative of the magnetic data showing a strong correlation between the fault trends from the seismic data and those from Euler's methods and the tilt derivative.

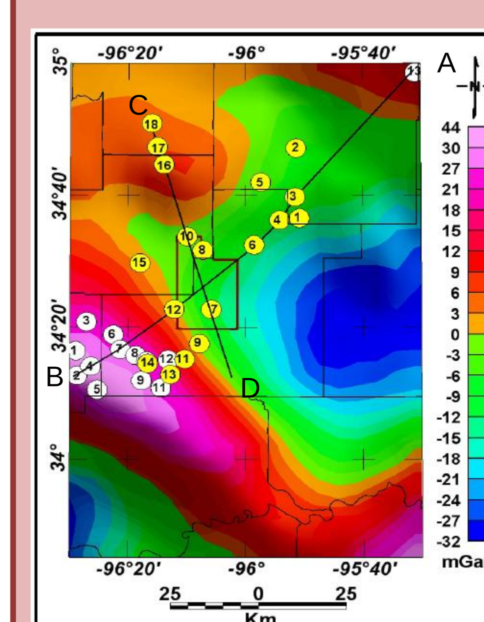

Fig. (18). Residual gravity map after upward continuation to 40 km shows the location of the wells and two selected profiles for the density models. Wells penetrate to the top of the basement are shown in white circles and those penetrate to the top of Arbuckle are shown in yellow circles.

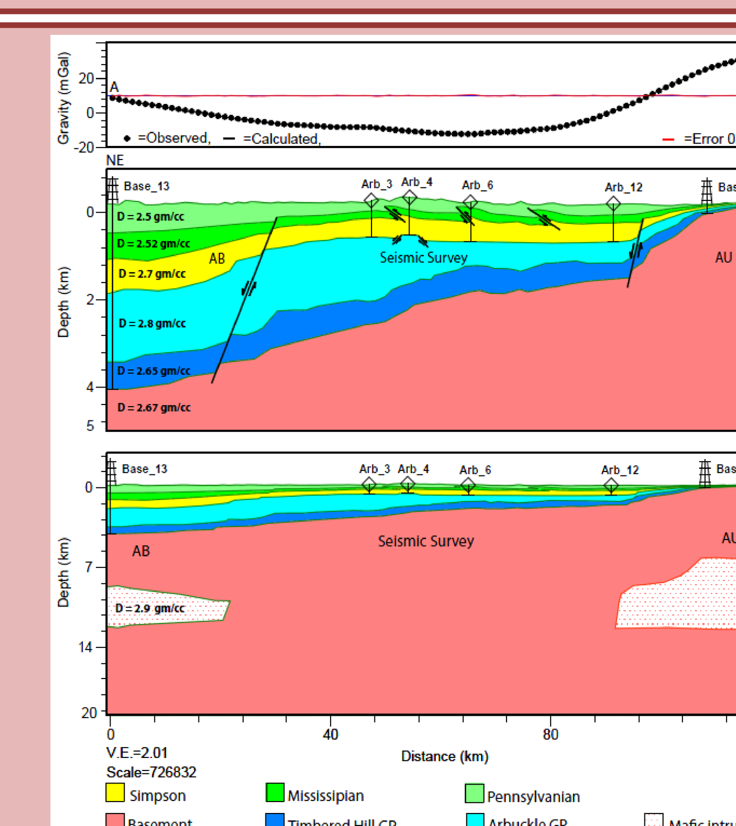

Fig. (19). Local gravity model along the profile AB. The positive anomaly at the southwest is due to mafic rocks at the core of Arbuckle Uplift (AU). The broad negative anomaly at the middle part coincide with the thickening of the thrusted Late Paleozoic strata and thickening of the Early Paleozoic rocks in Arkoma basin (AB). D refers to the densities of the different stratigraphic units. Arb_# and Base_# refer to the wells that penetrate to the top of the Arbuckle Group and basement, respectively.

Conclusion

- The basement rocks were subjected to severe and intense deformation as well as deep erosion.
- The structural interpretation reflects different styles of structural deformation influencing the study area. Normal faults dominate the basement and the Lower Paleozoic rocks while compressional structures dominate the Upper Paleozoic rocks.
- An EW zone of crustal weakness has been recognized in the northern part of the study area. The weakness zone represent a tectonic reactivation of the Cambrian rifting faults as compressional thrust faults of the Late Paleozoic Ouachita and/or Arbuckle orogeny.
- The basement structures clearly influenced the Paleozoic structures and the depositional history of the Arkoma basin.
- Seismic attributes, Euler solution cluster plot and edge detector techniques show and enhance the occurrence of the EW zone of the intensive deformation.
- Fault trends determined by the Euler depth estimation method show strong correlation to those obtained from seismic data.
- The maximum depth value of about 3850 m may represent faults that penetrate deeply into the basement or due to intra-basement features or structures.

References

- Arbenz J. Kaspar; 2008: Structural framework of the Ouachita Mountains. Oklahoma Geological Survey Circular 112A, PP. 1-40.
- Chopra S. and Marfurt K.; 2007: Seismic attributes for prospect identification and reservoir characterization.
- Sutherland K. Patrick; 1988: Late Mississipian and Pennsylvanian depositional history in the Arkoma basin area, Oklahoma and Arkansas. Geological Society of American Bulletin, v. 100, p. 1787-1802.

Acknowledgment

We would like to thank Cgg Veritas and PABLO ENERGY II, LLC for providing the 3D seismic data and giving permission to publish this work. We would like also to thank the Oklahoma Geological Survey staff especially Mr. Richard D. Andrews for providing well data. Seismic interpretation was done by Petrel software provided by Schlumberger for use in research and education.